

# Metallicity of ionized gas in the Irr galaxy IC10

Egorov O.V.<sup>1</sup>, Lozinskaya T.A.<sup>1</sup>, Moiseev A.V.<sup>2</sup>

<sup>1</sup>Sternberg Astronomical Institute, Moscow, Russia

<sup>2</sup>Special Astrophysical Observatory of Russian Academy of Science, Nizhnii Arkhyz, Karachai-Cherkessia, Russia

## Introduction

The dwarf irregular galaxy IC10 is the nearest starburst galaxy at the distance 800 kpc. H $\alpha$  and [SII] line images of this galaxy show a giant complex of multiple shells and supershells with sizes ranging from 50 to 500-800 pc (see Fig. 1). The stellar population of the galaxy and anomalously high space density of WR stars are indicative of almost "synchronous" and short burst of ongoing star formation, which, however, must have spread throughout most of the galaxy. It is the place where the currently most bona fide hypernova remnant - the Synchrotron Supershell - has been identified [1].

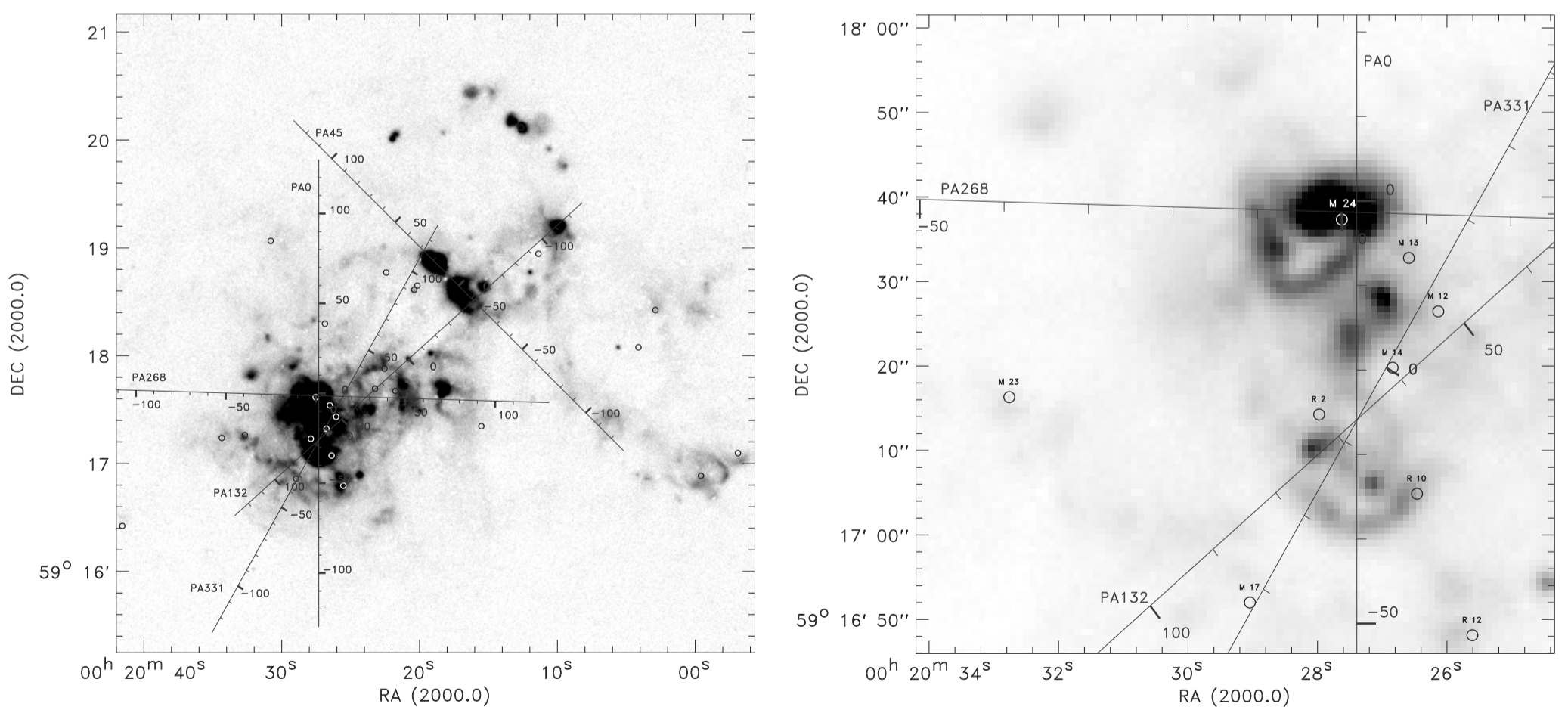


**Fig. 1a,b.** Location of slit spectrograms on the H $\alpha$ -line image of IC10. The circles indicate WR stars.

## Observations

The observations of the galaxy were performed at the 6-m telescope of the Special Astrophysical Observatory of the Russian Academy of Sciences. Five spectrograms named by their position angles - PA0, PA45, PA132, PA268 and PA331- were taken with SCORPIO focal reducer operating in the slit spectrograph mode. Figures 1a and b show the locations of the slit spectrograms on the  $H\alpha$ -line image of IC10 with the arc second marks superimposed. The scale along the slit and spectral resolution were equal to  $0,36''/\text{pixel}$  and about 5-9 Å, respectively.

## Relative abundances

Relative abundances of oxygen are derived using three methods. First one is the theoretical dependence of  $12+\log(\text{O}/\text{H})$  from  $[\text{OII}]\lambda 3727$  and  $[\text{OIII}]\lambda 4959+5007$  line intensities divided by  $H\beta$  line intensity, and from electronic density and temperature [2]. Second one is the revised calibration of  $12+\log(\text{O}/\text{H})$  as a function of  $[\text{OII}]$  and  $[\text{OIII}]$  line intensities [3]. And third method [4] is the dependence of  $12+\log(\text{O}/\text{H})$  from ratios  $\log([\text{OII}]\lambda 3727)/\log([\text{OIII}]\lambda 5007)$  and  $\log([\text{NII}]\lambda 6583)/\log([\text{SII}]\lambda 6717+6731)$ .

We have defined relative abundances of nitrogen and sulfur, using a method resulted in [2].

Figures 2, 3, 4 show the distributions of the inferred  $12+\log(\text{O}/\text{H})$ ,  $\log(\text{N}/\text{O})$ ,  $\log(\text{S}/\text{O})$  values along the slits; we averaged the abundances over HII regions from the catalog of Hodge and Lee [5]. The results are also summarized in the Table1. Columns 1, 2, 3, 4, 5 and 6 give the name of the region according to [5]; the position on the corresponding slit, and the inferred  $12+\log(\text{O}/\text{H})$  (first and second methods only),  $\log(\text{N}/\text{O})$ ,  $\log(\text{S}/\text{O})$  values, respectively.

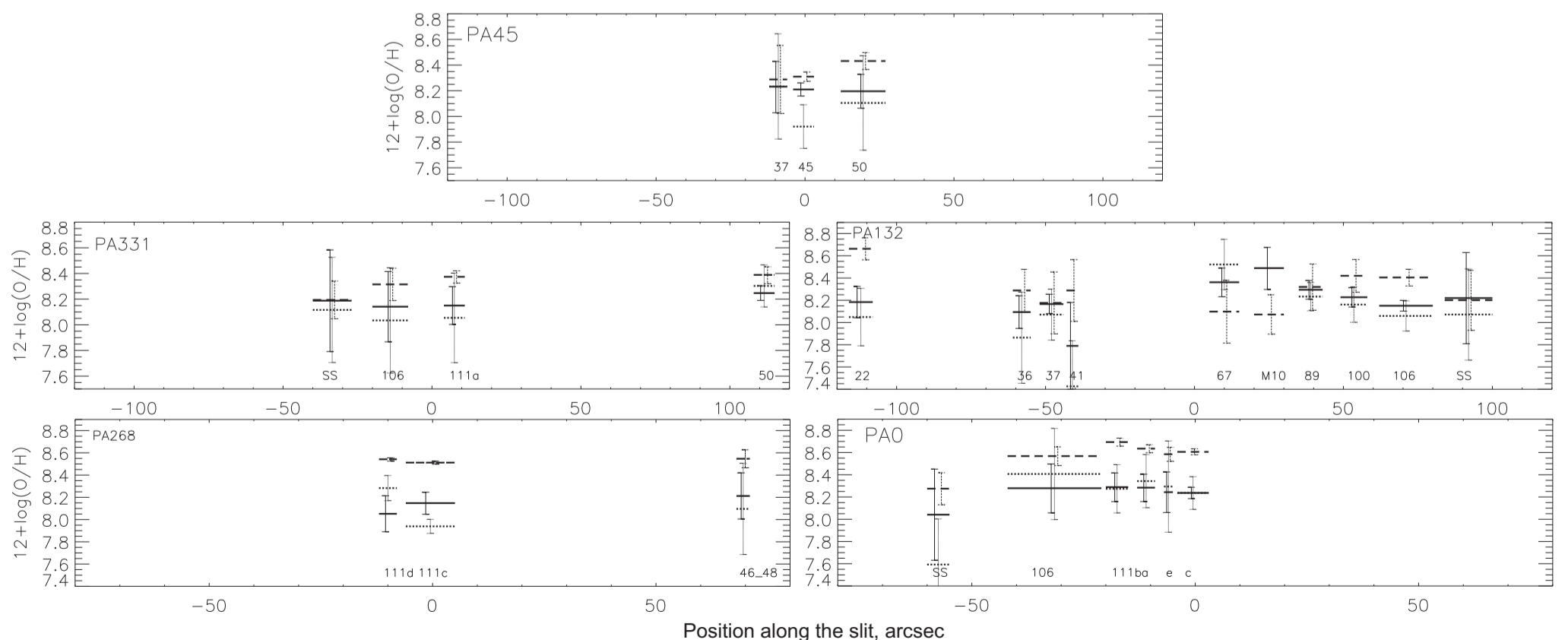


**Fig. 2.** Relative oxygen abundance along the slits. Solid line marks a first method [2] of abundance determination, dotted line – a second method [3] and dashed line – a third method [4].

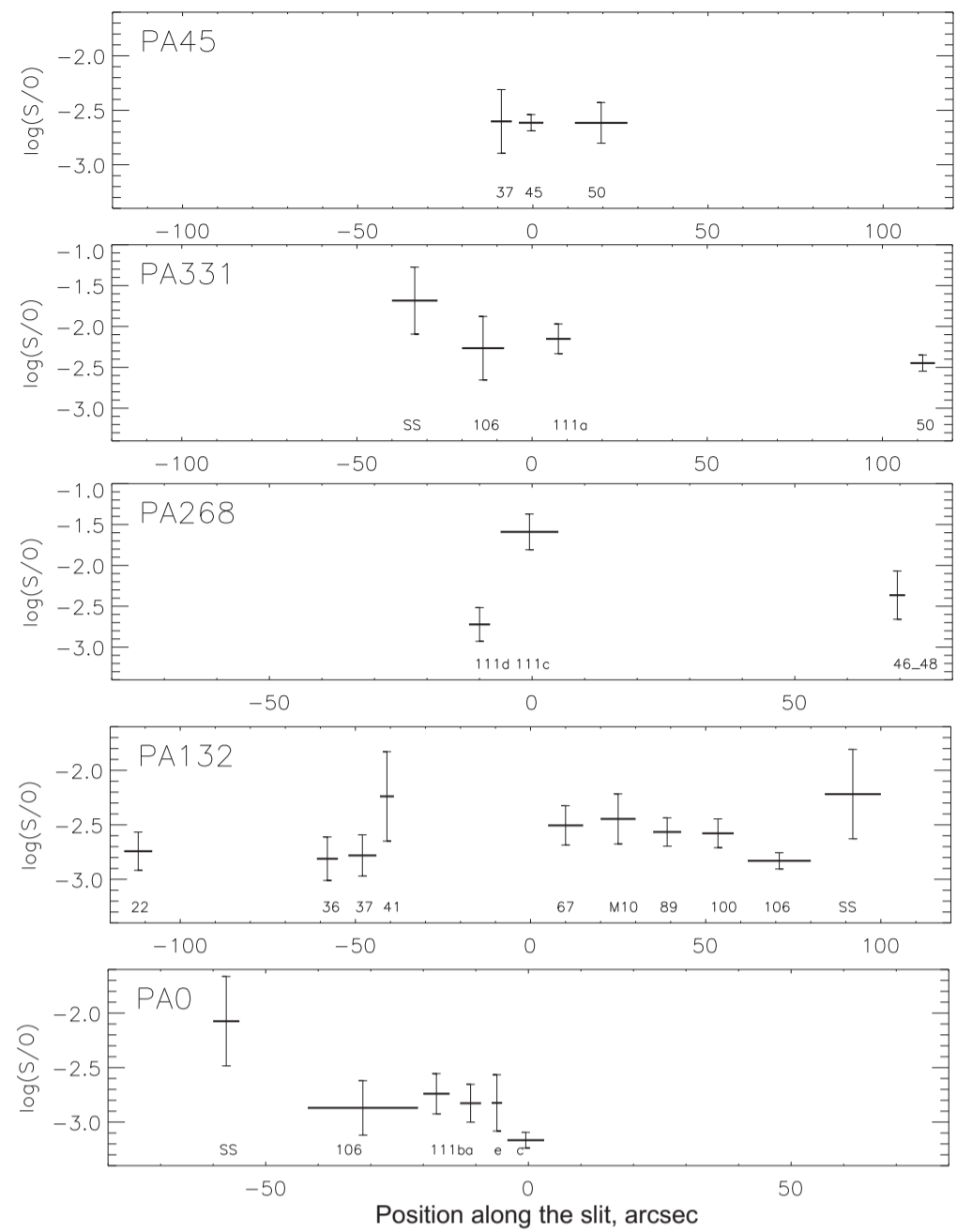
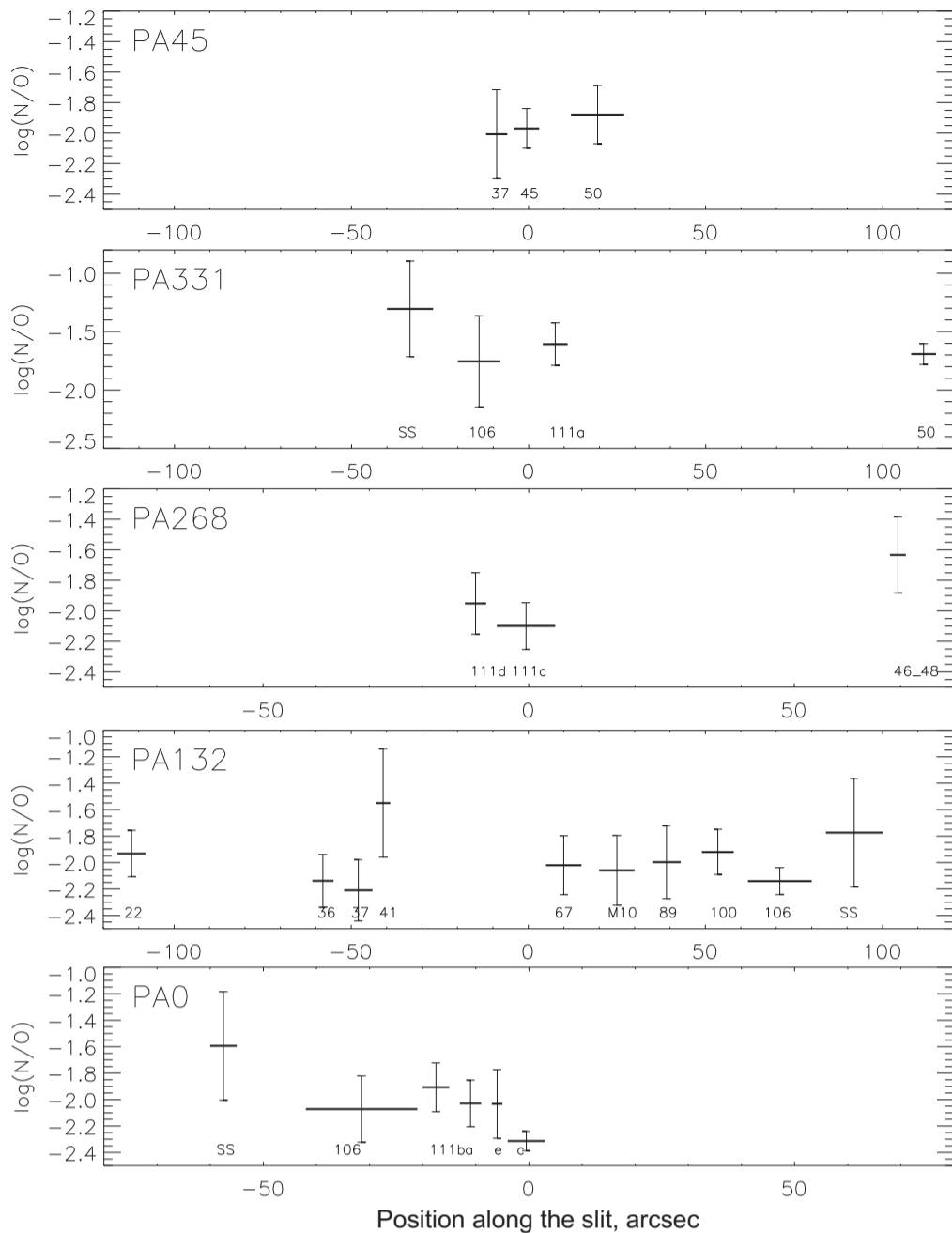


**Fig. 3.** Relative nitrogen abundance along the slits.

**Fig. 2.** Relative sulfur abundance along the slits.

**Table 1.** Relative abundances of O, N, S.

Region	Slit/Position	12+log(O/H) (1)	12+log(O/H) (2)	12+log(N/H)	12+log(S/H)
HL111a	PA0[-13, -9]	$8.34 \pm 0.24$	$8.28 \pm 0.12$	$6.26 \pm 0.13$	$5.46 \pm 0.12$
	PA331[4, 11]	$8.05 \pm 0.34$	$8.15 \pm 0.15$	$6.54 \pm 0.16$	$6.00 \pm 0.16$
HL111b	PA0[-20, -15]	$8.27 \pm 0.22$	$8.29 \pm 0.13$	$6.38 \pm 0.13$	$5.55 \pm 0.13$
HL111c	PA0[-4, 3]	$8.24 \pm 0.15$	$8.24 \pm 0.10$	$5.92 \pm 0.10$	$5.07 \pm 0.10$
	PA268[-6, 5]	$7.94 \pm 0.10$	$8.15 \pm 0.10$	$6.05 \pm 0.12$	$6.56 \pm 0.22$
HL111d	PA268[-12, -8]	$8.28 \pm 0.11$	$8.05 \pm 0.16$	$6.10 \pm 0.18$	$5.33 \pm 0.19$
HL111e	PA0[-7, -5]	$8.29 \pm 0.38$	$8.24 \pm 0.18$	$6.21 \pm 0.19$	$5.42 \pm 0.18$
HL106	PA0[-42, -21]	$8.41 \pm 0.42$	$8.28 \pm 0.22$	$6.21 \pm 0.22$	$5.41 \pm 0.22$
	PA132[62, 80]	$8.06 \pm 0.14$	$8.15 \pm 0.10$	$6.01 \pm 0.10$	$5.32 \pm 0.10$
	PA331[-20, -8]	$8.03 \pm 0.42$	$8.14 \pm 0.27$	$6.39 \pm 0.27$	$5.88 \pm 0.28$
SS	PA0[-60, -55]	$7.59 \pm 0.42$	$8.04 \pm 0.43$	$6.44 \pm 0.41$	$5.97 \pm 0.43$
	PA132[84, 100]	$8.07 \pm 0.18$	$8.22 \pm 0.21$	$6.45 \pm 0.38$	$6.00 \pm 0.41$
	PA331[-40, -27]	$8.12 \pm 0.42$	$8.19 \pm 0.39$	$6.88 \pm 0.39$	$6.50 \pm 0.39$
HL37	PA45[-12, -6]	$8.23 \pm 0.42$	$8.23 \pm 0.20$	$6.23 \pm 0.24$	$5.63 \pm 0.21$
	PA132[-52, -44]	$8.07 \pm 0.23$	$8.17 \pm 0.10$	$5.96 \pm 0.22$	$5.39 \pm 0.17$
HL45	PA45[-4, 3]	$7.92 \pm 0.17$	$8.21 \pm 0.10$	$6.24 \pm 0.12$	$5.60 \pm 0.10$
HL50	PA45[12, 27]	$8.10 \pm 0.36$	$8.20 \pm 0.13$	$6.32 \pm 0.14$	$5.58 \pm 0.13$
	PA331[108, 115]	$8.30 \pm 0.16$	$8.25 \pm 0.10$	$6.56 \pm 0.10$	$5.80 \pm 0.10$
HL100	PA132[49, 58]	$8.16 \pm 0.16$	$8.23 \pm 0.10$	$6.31 \pm 0.15$	$5.65 \pm 0.10$
HL89	PA132[35, 43]	$8.23 \pm 0.13$	$8.29 \pm 0.10$	$6.30 \pm 0.27$	$5.72 \pm 0.10$
M10	PA132[20, 30]	$8.74 \pm 0.36$	$8.49 \pm 0.19$	$6.43 \pm 0.29$	$6.04 \pm 0.20$
HL67	PA132[5, 15]	$8.52 \pm 0.23$	$8.36 \pm 0.13$	$6.34 \pm 0.20$	$5.86 \pm 0.17$
HL41	PA132[-43, -39]	$7.73 \pm 0.42$	$7.79 \pm 0.39$	$6.24 \pm 0.39$	$5.55 \pm 0.39$
HL36	PA132[-61, -55]	$7.86 \pm 0.42$	$8.09 \pm 0.15$	$5.96 \pm 0.19$	$5.28 \pm 0.19$
HL22	PA132[-116, -108]	$8.28 \pm 0.12$	$8.18 \pm 0.14$	$6.25 \pm 0.16$	$5.44 \pm 0.16$
HL46,48	PA268[68, 71]	$8.10 \pm 0.40$	$8.21 \pm 0.21$	$6.58 \pm 0.23$	$5.85 \pm 0.21$

## Discussion and results.

We reveal strong variations of *interstellar extinction* between different regions, which explain the discrepancies between early extinction and distance estimates for IC10. The observed variations may be due to "local" extinction in the central star-forming region, which resides in the direction of the densest cloud of neutral and molecular gas and is possibly partially embedded in it. We adopt  $E(B-V) = 0.95^m$  (our paper [6] in press) in this work.

Our results provide the currently most detailed *O, N and S relative abundance* data for the galaxy. Our measurements show the oxygen abundance to vary over a wide range from one region to another. The mean abundance averaged over the regions studied is  $12 + \log(O/H) = 8.17 \pm 0.35$ , that correspond to metallicity  $Z = 0.18 \pm 0.14Z_{\odot}$ . The oxygen abundance in the brightest region HL111 is, on the average, equal to  $12 + \log(O/H) = 8.25 \pm 0.19$ .

The line intensity ratio of  $I([SII])/I(H\alpha) = 0.7-1.0$  in the *Synchrotron Supershell* (SS in table and at the figures) is indicative of gas emission behind the shock. The latter is also evidenced by higher  $I([NII]6548+6583)/I(H\alpha) \simeq 0.25$  and  $I([OII]3727)/I([OIII]5007) \simeq 1.58$  ratios and lower  $I([OIII]5007)/I(H\beta) \simeq 0.15$  ratio compared to the neighboring HL106 bright HII region. The inferred estimate of oxygen abundance in the Synchrotron Supershell remains uncertain, because the compact hypernova remnant — IC 10 X-1 — is a binary consisting of a black hole and WR M17 star. Ionizing radiation of the WR star may be important in its neighborhood. On the other hand, shock must be taken into account for the technique used for HII to be correctly applicable in our case. We therefore derive provisional oxygen abundance estimates using three methods while being fully aware of the incorrectness of both approaches. Using the first method we find  $12 + \log(O/H) = 8.22 \pm 0.21$ ,  $12 + \log(O/H) = 8.04 \pm 0.43$  and  $12 + \log(O/H) = 8.19 \pm 0.39$  based on the spectrograms of PA132, PA0 and PA331 interpreted in terms of the HII region model. Our observations agree best with the models of [7] for the radiation of gas behind a shock propagating at a velocity of about 100 km/s ([8]) if we adopt  $12 + \log(O/H) \simeq 8.15$  for models of pure shock excitation or  $12 + \log(O/H) \simeq 8.35$  for models that allow shock pre-ionization of gas.

You can find more detailed results of our work in our paper [6].

This work is supported by the Russian Foundation for Basic Research (project no. 07-02-00227) and is based on observational material obtained with the 6-m telescope of the Special Astrophysical Observatory of the Russian Academy of Sciences funded by the Ministry of Science of the Russian Federation (registration number 01-43).

## References.

1. Lozinskaya T.A., Moiseev A.V., MNRAS, **381**, 26L (2007)
2. Izotov Y.I., Stasinska G., Meynet G., Guseva N.G., Thuan T.X., Astron.Astrophys.,**448**, No. 3, 955-970 (2006).
3. Pilyugin L.S., Thuan T.X., Astroph.J. **631**, 231 (2005).
4. Charlot S., Longetti M., MNRAS **323**,887 (2001)
5. Hodge P., Lee M.G., PASP, **102**, 26 (1990).
6. Lozinskaya T.A., Egorov O.V., Moiseev A.V., Bizyaev D.V., Astron. Lett. Vol **35**, №10, 730-747, in press (2009)
7. Allen M.G., Grovs B.A., Dopita M.A., Sutherland R.S., Kewley L.J., ASTRO-PH 0805.0204 (2008).
8. Lozinskaya T.A., Moiseev A.V., Podorvanyuk N.Yu., Burenkov A.N., Astron. Lett. **34**, No. 4, 217-230 (2008).